Fibroblast recruitment as a tool for ovarian cancer detection and targeted therapy

Roni Oren[1], Yoseph Addadi[1], Lian Narunsky Haziza[1], Hagit Dafni[2], Ron Rotkopf[3], Gila Meir[1], Ami Fishman[4] and Michal Neeman[1]

[1] Department of Biological Regulation, Weizmann Institute of Science, Rehovot, Israel
[2] Department of Veterinary Resources, Weizmann Institute of Science, Rehovot, Israel
[3] Department of Biological Services, Weizmann Institute of Science, Rehovot, Israel
[4] Department of Obstetrics and Gynecology, Meir Medical Center, Kfar Saba, Sackler School of Medicine, Tel-Aviv University, Israel

Metastatic ovarian cancer, the most lethal of gynecologic malignancies, is typically managed by debulking surgery, followed by chemotherapy. However, despite significant efforts, survival rate remains low. We have previously demonstrated, in mouse models, a specific systemic homing of labeled fibroblasts to solid ovarian tumors. Here, we demonstrate the feasibility of utilizing this specific homing of genetically modified fibroblasts for detection and targeted therapy of orthotopic metastatic ovarian carcinoma model in immune-deficient mice. Using an in vivo metastatic mouse model for ovarian cancer, we demonstrated that fibroblasts expressing fluorescent reporters injected intra-peritoneally, were specifically recruited to peritoneal tumor nodules (resulting in 93-100% co-localization). We further used fibroblasts over expressing the soluble receptor variant of VEGFR1 (s-Flt1). Mice bearing tumors were injected weekly with either control or s-Flt1 expressing fibroblasts. Injection of s-Flt1 expressing fibroblasts resulted in a significant reduction in the ascites volume, reduced vascularization of adherent metastases, and improved overall survival. Using fluorescently labeled fibroblasts for tumor detection with readily available intra-operative fluorescence imaging tools may be useful for tumor staging and directing biopsies or surgical efforts during exploratory or debulking surgery. Fibroblasts may serve as a beacon pointing to the otherwise invisible metastases in the peritoneal cavity of ovarian cancer patients. Utilizing the recruited fibroblasts also for targeted delivery of anti angiogenic or antitumor molecules may aid in controlling tumor progression. Thus, these results suggest a novel approach for targeting ovarian tumor metastases for both tumor detection and therapy.

Tumor Immunology and Microenvironment

Ovarian cancer is the most lethal gynecologic malignancy[1,2] with a mean five year survival after diagnosis of only 43.2%.[3] The poor prognosis may be due to the late stage at the time of diagnosis, when metastases are already widely spread.[4,5] Currently, available treatment options are limited, patients diagnosed with ovarian cancer are treated by debulking surgery followed by cytotoxic chemotherapy (platinum and taxane analogues).[6] Complete surgical removal of malignant tissue is critical for outcome and thus improved intraoperative imaging can have a significant benefit in surgical success.[5] Magnetic resonance imaging (MRI) and computed tomography combined with ultrasound are being used for pre-operative assessment of malignancies in patients, but are not useful for real time surgical guidance, and many times cannot detect very small metastasis. Fluorescence imaging however, has advantages in pre-clinical and clinical trials for real time imaging with high sensitivity and specificity using a variety of probes.[7–12] The first clinical trial in image guided surgery of ovarian cancer was conducted by van Dam et al. using intravenously administered folate-FITC. This study demonstrated an increase in tumor detection.[10,13] However there is still a need for improved specificity and sensitivity for targeting of fluorescent agents for guided surgery. The use of folate receptor for the detection of tumor lesions resulted in some false positive discovery rate of

What's new?

For patients with metastatic ovarian cancer, survival time is greatly influenced by the extent to which malignant tissue can be removed through debulking surgery. However, even with seemingly complete debulking, very small metastases frequently persist. This study shows that in mice, these otherwise invisible metastases can be identified with fluorescently labeled fibroblasts injected into the peritoneal cavity, where they are recruited specifically to tumor nodules. Mice treated with labeled fibroblasts genetically modified to express the soluble receptor variant of VEGFR1 (s-Flt1), a negative regulator of angiogenesis, benefited from suppressed ascitic fluid formation and prolonged survival.

23% in patients. This can significantly effect the surgical procedure and cause more extensive and un necessary intervention. In addition, folate receptor is expressed in 72% of primary tumors in ovarian cancer and in 81.5% of recurrent ovarian tumors[14] and there is a need to find supplementary method to match all patients with additional probes to other molecular or cellular targets. False positive detection can be dramatically reduced by targeting a unique probe or by taking advantage of a native biological process for the signal localization.

Ovarian tumors are characterized by relatively high contribution of stromal cells including fibroblasts, immune cells, endothelial cells and others, with a median of 50% of the tissue composed of stromal cells, not depending on stage or histotype.[15] In both clinical specimens and mouse models, stroma is the major component of the ovarian tumor. Ovarian cancer is also characterized by the accumulation of ascitic fluid in the abdominal cavity and metastatic spread to the peritoneal surfaces.[16,17] More than a third of ovarian cancer patients will develop ascites during their disease which may involve tumor cells, fibroblasts, macrophages, mesothelial cells and white and red blood cells.

Cancer associated fibroblasts (CAF) are a dominant compartment in the tumor stroma and have been shown to be involved in tumor progression and metastasis.[18] Fibroblasts have a dual role in tumor progression. Normal fibroblasts inhibit preneoplastic growth in normal tissues. However, in response to oncogenic stimuli, fibroblasts can also act to promote tumor progression by leading and stabilizing tumor angiogenic vasculature and facilitate invasion and migration of cancer cells.[19,20] We have previously demonstrated in a subcutaneous tumor xenograft model, that exogenously administered fibroblasts are recruited specifically to the ovarian carcinoma vasculature.[21,22] These recruited fibroblasts were activated to form myofibroblasts (namely, expressing α-SMA).[21] The ability to use normal and abundant cells such as fibroblasts, to target tumors, opens possibilities for targeted imaging and therapy.[23–25]

VEGF signaling was shown to regulate ascites formation in ovarian cancer. Mesiano *et al.* demonstrated inhibition of ascites formation in a mouse model by immunoneutralization with anti VEGF antibody.[26] They also showed that VEGF activity is necessary for ascites formation, but not for tumor growth. VEGF has a higher affinity towards VEGFR1 compared with VEGFR2, but VEGFR1 activation has a lower impact on signal transduction due to a weak tyrosin kinase activity.[27,28] Through alternative splicing, VEGFR1 encodes a soluble variant (sFLT-1), which consists of an extra cellular domain of VEGFR1. sFLT-1 is more efficient than membrane bound VEGFR1 in binding VEGF, and therefore can serve as a VEGF trap.[29,30] Importantly, sFlt-1 expression by ovarian cancer tumor cells, in a mouse model, resulted in suppression of ascites accumulation and prolonged survival.[26,31]

Therefore in this study, we aimed to use the specific recruitment of fibroblasts as a multifunctional tool, not only to highlight tumors, but also for localized delivery of sFLT-1 to the tumor. We hypothesized that local inhibition of VEGF activity by sFlt-1 expression in peri-vascular fibroblasts at the tumor sites could provide an effective avenue to control ascites formation and angiogenesis in ovarian cancer while decreasing the systemic exposure to suppression of VEGF signaling. Here we demonstrate that fibroblasts expressing sFlt-1 are specifically recruited to tumor sites, and indeed significantly suppress the amount of ascites accumulated in the mice, reduced tumor angiogenesis and improved overall survival.

Material and Methods
Cell culture
CV1, normal monkey kidney fibroblasts (ATCC) and ES2, human ovarian epithelial carcinoma cells (ATCC) were grown in DMEM supplemented with 10% FBS. SKOV3 cells (ATCC) were cultured in RPMI supplemented with 10% FBS. MRC5sv, SV40-transformed human lung fibroblasts (kindly provided by Prof. Zvi Livneh from the Weizmann Institute and originally obtained from Dr. Alan R. Lehmann) were cultured in minimum essential medium (MEM Eagle; Biological industries) supplemented with 15% FBS (Biological industries). All media were also supplemented with 1% pen-strep solution and 1% L-glutamine (Biological industries) and cells were maintained in 5% CO_2, 95% air at $37°C$.

Generation of ES2 spheroids was done by seeding 3×10^6 cells on agar-coated $75 cm^2$ flasks for 4 days. Prior to inoculation into mice, spheroids (~ 100 μm in diameter) were collected, washed in PBS and counted.

SKOV3 spheroids were created by seeding the cells in hanging drops (8,000 cells/25 μl) in culture medium containing 2.4% (final concentration) carboxymethylcellulose (Methocel,

Tumor Immunology and Microenvironment

Sigma) as described by Laib *et al.*[32] The spheroids were collected and washed in PBS prior to injection into mice.

For conditioned medium experiments, tumor and fibroblast cells were seeded at 10^6 cells/10 cm plate. The following day medium was changed with fresh medium. Forty-eight hours later the conditioned medium was collected, centrifuged to remove cell debris and used as growth media for fibroblasts or cancer cells for additional 48 hr.

RNA preparation, qRT-PCR
RNA was prepared using RNeasy kits according to manufacturer protocol (QIAGEN). One microgram of RNA was reverse transcribed using High capacity reverse transcription kit according to manufacturer protocol (Applied Biosystems). qRT-PCR was performed using SYBR fast Master mix (Roche) on LightCycler480 instrument (Roche).

The following primers (Sigma) were used (from 5' to 3'): GAPDH AGGGCTGCTTTTAACTCTGGT and CCCCACTT GATTTTGGAGGGA, B2M TTCTGGCCTGGAGGCTATC and TCAGGAAATTTGACTTTCCATTC, VEGF-A CCAGG CCCTCGTCATTG and AAGGAGGAGGGCAGAATCAT, VEGF-C TGCCAGCAACACTACCACAG and GTGATTA TTCCACATGTAATTGGTG, SDF1 TCAGATTGTAGCCC GGCTGAAGA and AGCGGAAAGTCCTTTTTGGCTGT, bFGF CACATTTAGAAGCCAGTAATCT and CCCGAC GGCCGAGTTGAC, αSma CACCATCGGAAATGAACG TTT and 5' GACTCCATCCCGATGAAGGA, Mmp1 CTGG CCACAACTGCCAAATG and CTGTCCCTGAACAG CCCAGTACTTA, Mmp2 GGGACAAGAACCAGATCACA-TACAG and TCCAGATCAGGTGTGTAGCCAAT, Mmp9 GGGACGCAGACATCGTCATC and TCGTCATCGTCG AAATGGGC uPA CACGCAAGGGGAGATGAA and CACG CAAGGGGAGATGAA.

The target messenger RNA (mRNA) expression level was calculated as the ratio of the target mRNA to GAPDH and B2M mRNA for each sample.

Expression vectors and stable transfections
ES2, CV1, SKOV3, and MRC5 cells were transfected to express fluorescent reporter proteins (GFP or Tomato) on a backbone of pIRES vector, under the EF-1a promoter.[33] Stable transfections were carried out with Lipofectamine 2000 reagent (Invitrogen), and 48 hr after transfection, puromycin (2.5 mg/ml; Sigma, St. Louis, MO) was added to initiate selection. Cells were maintained on same concentration of antibiotics after selection in order to maintain reporter gene expression. Selection was confirmed by fluorescence microscopy at all stages.

MRC5 cells were transfected to express sFlt1. The sFlt1 sequence (GenBank: D88690.1) was reverse-transcribed from mouse placenta mRNA and PCR-amplified using Phusion high-fidelity DNA polymerase (Finnzymes, Espoo, Finland). The following forward and reverse primers (Sigma) were used, ACCATGGTCAGCTGGGAC and TTAATGTTTGA-CATGACTTTG. The fragments were ligated into pCR-

BluntII-TOPO (Invitrogen), and their sequence fidelity was confirmed by DNA sequence analysis. Inserts were restricted and ligated into pIRES expression vector containing the human EF-1a promoter.[34]

Animal model
All animal procedures were approved by the Weizmann Institutional Animal Care and Use Committee. 7- to 8-week-old CD-1 nude female mice (Harlan laboratories, Israel) were used in all experiments.

For *in vivo* fluorescence imaging, the regular chow provided to the mice was replaced with chlorophyll free chow (Harlan laboratories, Israel) for at least 3 days prior to imaging, in order to reduce background auto-fluorescence.

Prior to tumor cell inoculation, mice were anesthetized by intra peritoneall injection of a mixture of 100 mg/kg ketamine and 20 mg/kg xylazine (Fort Dodge Animal Health); and 100–300 ES2 or SKOV3 spheroids were injected intra peritoneally[35,36] to the left side of the abdomen using a 21G needle. Fibroblasts ($2-4x10^6$) were administered 5–7 days later by intra peritoneal injection to the contra-lateral abdominal side. For co-localization analysis of tumor and fibroblasts, all tumor nodules and fibroblasts in the mice were counted and marked ex vivo using fluorescence stereo-microscope.

For s-Flt1 treatment, mice bearing intraperitoneal tumors were injected weekly with s-Flt1 expressing fibroblasts or control fibroblasts. For ES2 the experiment was terminated 3 weeks after tumor initiation and ascites volume was collected and measured with a 1-ml syringe. Tumor burden in peritoneal cavity was scored with fluorescence stereo-microscope by an observer blinded to the treatment groups. For overall survival (ES2 and SKOV3), the animals were monitored regularly until morbidity or euthanized according to institutional ethical guideline.

For subcutaneous tumors $4x10^6$ ES2 cells were injected alone or mixed with MRC5 fibroblasts cells. Tumor size was measured with caliper after 21 days.

Window chamber/dorsal skin fold chamber
Titanium dorsal window chamber was used for intravital fluorescence microscopy (Research Instruments, Durham, NC).

Mice were surgically implanted with the window chamber under anesthesia according to standard procedure as previously described.[37] The procedure was performed on a heated platform, under sterile conditions. Mice were given 24–48 hr to recover in a heated environment (30°C) before tumor inoculation into the chamber. Subcutaneous chamber tumors were generated by inoculation of 2–5 $x10^6$ cells suspended in a total volume of 30 μl into skin in the window area of the mouse under anesthesia. CV-1 Tomato fibroblasts were injected IP ($2x10^6$ cells in 30 μl of PBS) 5–7 days following tumor inoculation.

Blood vessel labeling in chamber experiments

DiD is a lipophilic dye (molecular probes; Exitation – 644 Emission 665). DiD was prepared as 2 mg/ml stock solution in 100% ethanol. Dilution in mix of ethanol: Cremophor EL (Sigma): PBS at 1:1:18 volume ratio, resulted in final concentration of 0.1 μg/ml.[38] A total volume of 200 μl was injected IV and imaged with two photon microscope.

Histological analysis

Diaphragm tissues retrieved from mice, were fixed at the end of the experiment with 2.5% PFA for 48 hr followed by 48 hr in 1% PFA and then 70% ethanol and embedded in paraffin blocks. Sections (3–5 μm) were stained for haematoxylin and eosin and immune stained using CD34 (Cedarlane Laboratories, 1:100) antibody for blood endothelial cells, antibody for s-FLT1 (Invitrogen, 1:100). Images were acquired with Zeiss Axio observer microscope equipped with a fluorescence illuminator and an Olympus DP72 camera. Acquired images were processed using ImageJ (National Institutes of Health; http://rsb.info.nih.gov/ij/). For CD34 analysis images of area from the diaphragm containing mainly tumor mass was imaged, CD34 coverage area was analyzed and compared between groups.

Imaging

Ex vivo stereomicroscope imaging of peritoneal cavity was performed on a fluorescent zoomstereo microscope SZX12 (Olympus, Japan) coupled with a CCD camera PIXELFLY QE, 12 bit (PCO, Germany).

Two photon microscopy

Two photon microscopy was performed using an LSM 510 META NLO microscope (Zeiss, Germany) equipped with a Broad Band Mai Tai – HP – Femtosecond single box tunable Ti-Sapphire oscillator, with automated broad band wavelength tuning 700–1020 nm from Spectraphysics, USA, for two photon excitation. Imaging was performed through a plan-Apochromat 20X/0.8 and plan-Apochromat[39] lens. Excitation – 850/890 nm, Emission beam was split by beam splitters, main beam splitter KP-650 and NDD_DBS1: FT:560, and collected by normal or non-descanned detectors BP 500–550 (GFP) BP 575–640 (Tomato) and BP390-465 (Second Harmonic). Imaged area – x: 420.84 μm, y: 420.84 μm.

Ex vivo two photon microscopy - Tumors were excised from the peritoneal cavity.

In vivo two photon microscopy - Mice bearing window chambers were placed in a fixed position on a xy motorized stage and imaged through the chamber.

Patient-derived ascites samples

Ascites samples were collected with the approval of the IRB committee of Meir Medical Center, Kfar-Saba, Israel. Fresh ascites was collected from patients ($n = 4$) with confirmed diagnosis of high-grade serous ovarian cancer during debulking surgery or peritoneal paracentesis. Samples were kept in suspension culture in DMEM supplemented with 10% FBS, 1% pen-strep solution and 1% L-glutamine in a 500-ml spinner flask (Belco, Vineland, NJ) at a spinning rate of 80 rpm. A mixture of 95% air and 5% carbon dioxide was blown over the medium for 5 min before the spinner was sealed and incubated at 37°C. On the next day, fluorescently labeled CV1 fibroblast (see below) were added to the cultured ascites. Images were acquired starting from 24 hr—4 days after fibroblast addition.

Patients pathology:

- Patient1 Primary peritoneal CA stage IIIC
- Patient2 Serous papillary cysadenofibroma
- Patient3 Primary peritoneal CA
- Patient4 Primary peritoneal CA stage IIIC

ELISA measurement of s-Flt1 in cells and plasma

Supernatant from MRC5 expressing s-Flt and control cells was collected. For measurement of s-FLT1 levels in the circulation, blood was collected from the retro-orbital sinus, under anesthesia. Plasma was separated by centrifugation and s-FLT1 levels were measured. s-FLT1 levels were measured using Mouse VEGF R1/Flt-1 Quantikine ELISA Kit (R&D) according to manufacturer's protocol.

Migration assay

Transwell chambers for 24-well plates were used, with 8-μm pores (Corning). CV1 cell migration towards ES2 or CV1 conditioned medium cells were seeded 2×10^5 cells/well in 24-well plates. Conditioned medium was collected after 24-hr incubation, spun down and placed in fresh 24-well plates. Transwell membranes were coated with 5 μg/ml of gelatin and 5×10^5 CV1 cells were seeded on each membrane. Cells were allowed to migrate for 6 hr at 37°C. After which membranes were fixed in 4% PFA, the upper side of the membrane was scraped to remove cells which had not migrated through the membrane. Membranes were stained with Hoechst (Invitrogen, 10 μg/ml), washed with PBS extensively and mounted on microscope slides. The experiment was performed in 4 repeats. For each repeat 6 fields were taken in a X10 magnification. Cell migration was quantified by ImageJ.

Proliferation assay

The 3−(4,5-dimethylthiazol-2-yl)−2,5-diphenyltetrazolium bromide (MTT, Invitrogen) assay was performed. Briefly, cells (2×10^3 cells in 100 μl per well) were plated in 96-well plates (flat-bottomed plate) and incubated with conditioned medium from tumor or fibroblasts cells. Cell viabilities were determined after 48, 72, and 96 hr.

Statistical analysis

Data is presented as indicated mean ±SEM. An independent, two-tailed, unpaired Student's *t test* was applied for analysis
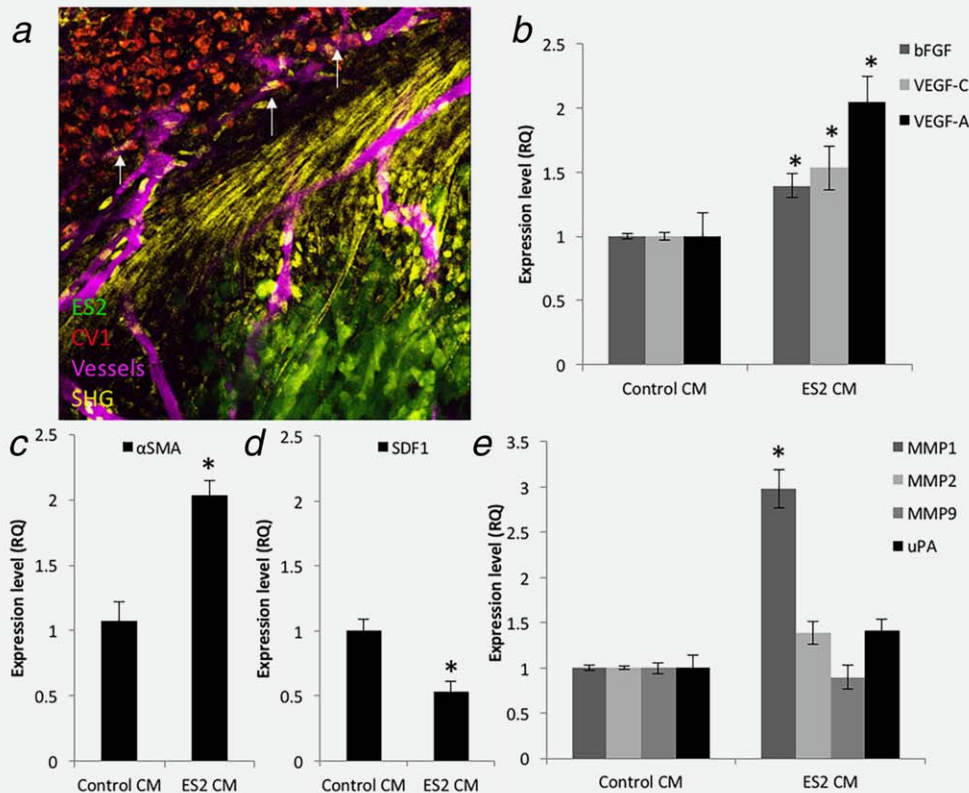
Figure 1. Fibroblasts recruitment to tumor cells is associated with blood vessels *in vivo* and fibroblasts are affected by tumor conditioned medium *in vitro*. (*a*) Maximal Intensity Projections (MIP) of a representative 2- photon stack of *in vivo* ES2 tumor (green) imaged in a dorsal window chamber model. CV-1 Tomato fibroblasts (Red) were injected IP 7 days after tumor inoculation and specifically recruited to the tumor within 24–48 hr. Tumor was imaged looking at cell populations, blood vessels (Magenta) and second harmonic generation (SHG) (Yellow) showing collagen fibers. Recruited fibroblasts are situated in close proximity to the angiogenic vessels (white arrows) at the tumor borders. Vessels morphology differs between tumor area and fibroblast area, the border is marked by the fibrotic "capsule" - yellow, comprised of ECM – collagen fibers and fibroblasts cells. Imaged area is 420.84 μm X 420.84 μm. (*b*−*e*) Real time PCR analysis of CV1 cells treated with ES2 tumor conditioned medium or control medium for 48 hr for pro-angiogenic factors (VegfA, VegfC and bFGF (*b*) αSMA (*c*), SDF1 (*d*), and ECM remodeling factors (MMP1, MMP2, MMP9 and uPA, (*e*). Expression level is reported as fold change (average of 4 experiments) ± standard error,* indicates *p*-value < 0.05.

of the significance of difference between groups. *t*-tests were conducted in Excel. The survival analysis was conducted with a Cox proportional hazards model, using the "survival" package in R (reference https://cran.r-project.org/web/packages/survival/citation.html). The data were considered to indicate a significant difference when *p* values were less than 0.05 and indicated in the text.

Results

Fibroblast recruitment to tumor cells was associated with blood vessels *in vitro* and *in vivo*

Fibroblast recruitment to tumors in subcutaneous models of ovarian cancer was previously reported.[21,22] Intravital microscopy showed that fluorescently labeled fibroblasts were recruited mainly to the ES2, human epithelial ovarian carcinoma, tumor rim and were aligned along blood vessels (Fig. 1*a*, arrows, Supporting Information Movie 1). The tumor region and fibroblast region seemed separated by a border marked by the fibrotic (collagen) "capsule" formed around

the tumor. This recruitment was consistent with our previous studies showing that the systemic recruitment is specific and unique to the tumor area.

Non-cell-autonomous signaling between tumor and stroma cells was evaluated using conditioned medium. Fibroblast cells were cultured in medium collected from ovarian tumor cells or medium conditioned by fibroblasts as a control. Measurement of gene expression revealed significant induction of angiogenic signaling. We found that culturing fibroblasts in medium collected from tumor cells induced transcription of VEGFA, VEGFC and basic fibroblast growth factor (bFGF) (Fig. 1*b*, *p* values < 0.05). Conditioned medium induce the expression of α-SMA a hallmark gene for activation of fibroblasts by tumor cells (Fig. 1*c*, *p* values < 0.05),[36] the upregulation of α-SMA goes in line with the expression of α-SMA in recruited fibroblasts as previously reported.[21,40] Stromal cell-derived factor-1 (SDF1) is a secreted factor involved in different aspects of the tumorigenic process including proliferation, survival, motility, migration, invasion
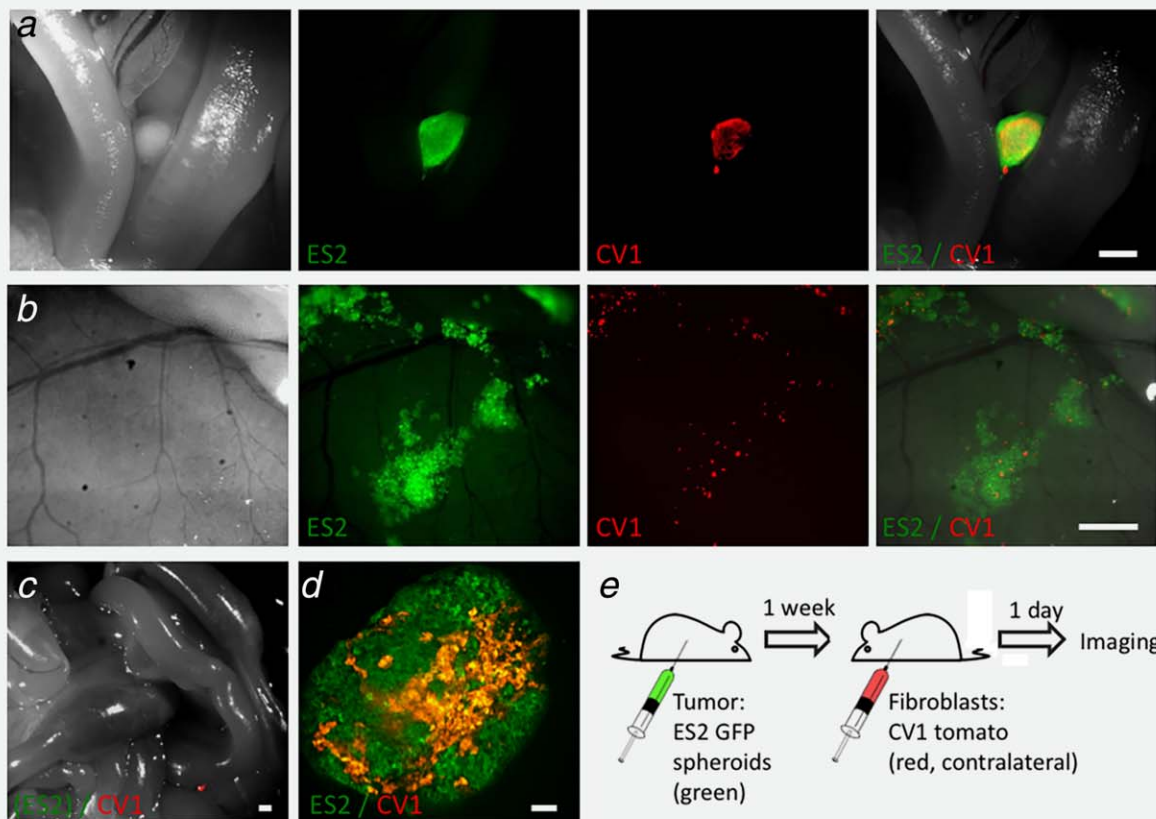
Figure 2. *In vivo* fibroblasts recruitment to ovarian ES2 micro metastases. ES2 spheroids (green) were injected IP to the left side of the abdomen. One week later CV1 -Tomato fibroblasts (red) were injected IP in the other side of the abdomen. One day after CV1 injection mice were sacrificed, abdomen was opened and imaged using stereo microscope. (*a,b*) Fibroblasts recruitment to tumor nodule next to intestine (*a*) and tumor patches attached to the peritoneal/abdominal wall (*b*). (*c*) Scattered fibroblast(s) in the abdomen of control mouse in which tumor was not injected. Scale bar (a-c) 1 mm. (*d*) High resolution image of recruited fibroblasts to tumor nodule (MIP, two photon microscopy). Scale bar 100 μm. (*e*) A scheme describing the experimental design.

and metastasis and recruiting endothelial cells and angiogenesis.[41] In response to conditioned medium we found that fibroblasts down regulated the expression of SDF1 (Fig. 1*d*, *p* values < 0.05). We also measured changes in genes involved in ECM remodeling and found matrix metalloproteinase 1 (MMP1) to be upregulated in response to conditioned medium, and no change in the expression of MMP2, MMP9 and uPA (Fig. 1*e*, *p* values < 0.05). Tumor conditioned medium did not change the proliferation rate or migration of fibroblasts (Supporting Information Fig. S1).

Specific fibroblasts recruitment to intraperitoneal ovarian ES2 micro metastases

In view of the recruitment of fibroblasts to solid subcutaneous ovarian tumor xenografts, we wanted to better model the clinical manifestation of ovarian tumor, and further test whether they could be recruited to the tumor in an orthotopic model of metastatic ovarian carcinoma. For that end, female CD-1 nude mice were inoculated intra-peritoneally with fluorescent GFP-expressing human ES2 ovarian carcinoma spheroids. Seven days after tumor initiation, tomato-expressing fluorescent CV1 fibroblasts were injected intra-peritoneally

(to the contra-lateral side of the abdomen). The mice were sacrificed and imaged one day after fibroblasts injection (Fig. 2). The fluorescence generated by the two reporter genes was used to detect tumor and fibroblast cells respectively. Injected tumor spheroids attached to the abdomen in multiple locations, and specific homing of the fibroblasts to tumor nodules and aggregates could be detected (Figs. 2*a* and 2*b*). In control animals in which no tumor was injected, very low residual fibroblasts signal could be detected, suggesting the effective clearance of non-adherent fibroblasts in the absence of tumor (Fig. 2*c*). No fibroblasts could be detected in other organs (including liver, lungs, omentum). Similar results were obtained in an additional fibroblast cell line, MRC5 (Supporting Information Fig. S2). The specific recruitment of fibroblasts to tumor nodules was also seen in SKOV3 tumor spheroids injected to mice (Supporting Information Fig. S3) and in solid tumors of both ES2 and MLS cells.[21] Higher magnification of a tumor nodule with recruited fibroblasts, showed the attachment of the fibroblasts to the tumor cells and infiltration into the tumor nodule (Fig. 2*d*).

The fibroblasts highlighted almost all of the tumor nodules with high selectivity and specificity (Table 1).

Tumor Immunology and Microenvironment

Table 1. Quantification of fibroblasts recruitment to ovarian ES2 micro metastases

Mouse #[1]	Co-localization[2]	Tumor only	Fibroblasts only	% of fibroblasts co localized
m1	289	10	8	97
m2	75	5	1	99
m3	41	4	3	93
m4	27	3	1	96
m5	88	13	1	99
m6	185	19	0	100
m7	215	8	2	99
m8	No tumor		4	
m9	No tumor		5	
m10	No tumor		17	
m11	No tumor		38	
m12	No tumor		14	
m13	No tumor		6	
m14	No tumor		3	

[1]Tumor-inoculated (m1-7) and control (m8-14) mice were sacrificed 1 day after CV1 fibroblast injection. Abdomen was opened and imaged using Olympus SZX12 stereomicroscope.
[2]Tumor nodule counted according to green fluorescence of ES2 GFP. Fibroblasts counted according to red fluorescent CV1-tomato. Co-localization was defined as number of green tumor nodules associated with red fibroblasts.

Quantification of fibroblast recruitment demonstrated that 93–100% of the total detectable fibroblasts were co-localized with tumor nodules (Table 1). The fibroblast cells could be detected at the tumor site as early as 1 day after their injection and were still visible 4 days after injection (data not shown). The detection of tumors using the fibroblasts gave low false negative (tumors with no adhered fibroblasts; 8.5%) and very low false positive (fibroblasts attached in the absence of a tumor; 2.4%). Thus, we achieved very high selectivity and high specificity for detection of tumors, by intra-operative fluorescence imaging, including very small, avascularized clusters of tumor cells, through the use of exogenously labeled fibroblasts.

Fibroblasts are recruited to fresh mouse ascites and human ascites *in vitro*

Fibroblasts affinity towards ovarian carcinoma was also tested using fresh patient-derived carcinoma specimens. Ascitic fluid specimens were collected from four ovarian cancer patients during de-bulking surgery or ascitic fluid drainage. The fluid was maintained in suspension culture for 24 h after collection. Fluorescently labeled CV1 fibroblasts were then added to the culture medium and the co-cultured cells were observed by fluorescence microscopy (Fig. 3). Cultured ascitic fluid formed tumor clusters with a spheroid like morphology. The labeled fibroblasts adhered to the tumor clusters and remained viable and adherent throughout the experiment, 5–
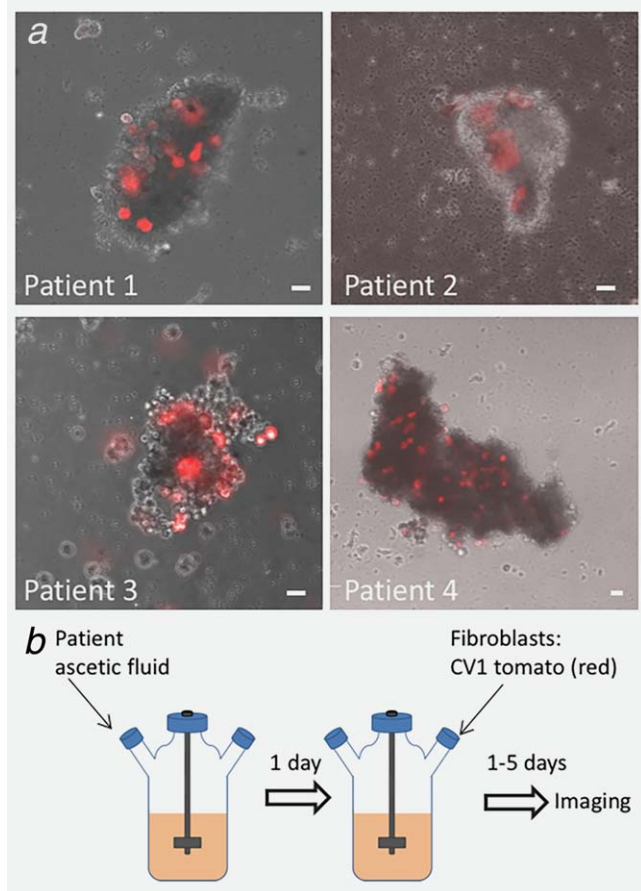

Figure 3. Fibroblasts recruitment to fresh human ascites *in vitro*. (*a*) Cultured patient-derived ascitic fluid formed spheroid-like tumor clusters. Co-culturing with CV1 fibroblasts (red) resulted in specific adherence of the fibroblasts to the tumor clusters (the images are from different patient-derived samples). (*b*) A scheme describing the experimental design. Scale bar 100 μm.

7 days of co-culture (Fig. 3). In order to compare the adherence of the fibroblasts to tumor cell aggregates from human-derived ascites to that of ascites of mouse origin, mouse ascitic fluid was collected 14 days after intraperitoneal injection of fluorescently-labeled ES2 cells. The adherence in both ascitic sources was comparable (Fig. 4). Suspension culture and co-culturing with fibroblasts did not affect spheroid morphology of the ascites-derived ES2 clusters, and again, adherence of fibroblasts to ovarian carcinoma cells was observed (Fig. 4).

s-Flt1-expressing fibroblasts attenuate ascitic fluid formation and improve survival

We further explored the feasibility of therapeutic utilization of the specific homing of labeled fibroblasts to ovarian tumors. First, we validated the contribution of fibroblasts to tumor growth. Endogenous fibroblasts are recruited by tumor cell from the surrounding neighborhood and mesenchymal stem cells are recruited from the bone marrow to become cancer associated fibroblasts. As previously reported,
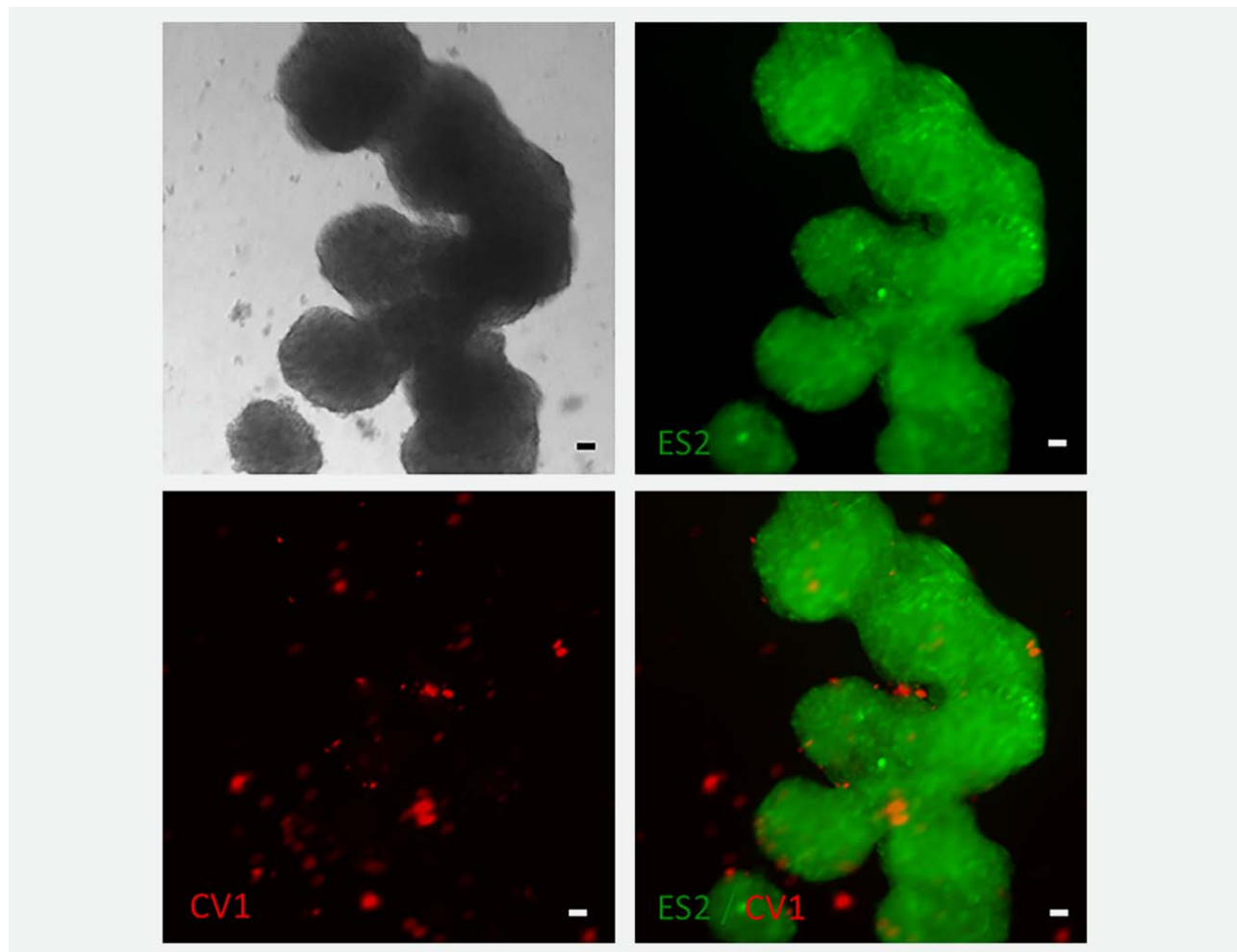
Tumor Immunology and Microenvironment

Figure 4. Fibroblasts recruitment to fresh mouse ascites *in vitro*. ES2 spheroids (green) were injected IP to the abdomen of mice, 14 days later mice were euthanized, and ascites fluid was collected and cultured. Co-culturing with CV1-Tomato fibroblasts (red) resulted in specific adherence of the fibroblasts to the tumor clusters. Scale bar 100 μm.

exogenously administered fibroblasts add only a small contribution to the endogenous tumor stroma (Granot Cancer Res[21]). Due to the difficulty in assessing tumor burden for peritoneal metastasis model we used the subcutaneous model. Co injection of fibroblasts with tumor cells subcutaneously to mice did not change tumor volume compared with tumor cells injected with no fibroblasts (Supporting Information Fig. S4). No inhibitory or stimulatory effect of fibroblasts on tumor growth rate was also reported in PC3 prostate cancer-derived cells tumor model.[42]

The association of the recruited fibroblast with blood vessels in the dorsal tumor model (Fig. 1*a*) prompted us to utilize the fibroblasts for suppression of angiogenesis by local targeting of VEGFA around the tumors. For that purpose we have generated fibroblasts cells that over express s-Flt1. The expression of s-Flt1 was validated by ELISA assay (Supporting Information Fig. S5). Mice bearing ES2 tumors were injected weekly (at Day 7 and Day 14) with either control or s-Flt1 expressing MRC5 fibroblasts. In order to assess the influence of s-Flt1 expressing fibroblasts on angiogenesis in

infiltrating metastasis, we analyzed the tumor region in the diaphragm of treated mice, and measured the coverage area of newly formed blood vessels as stained with CD34 antibody (Figs. 5a and c). We found a significant decrease in the amount of newly formed blood vessels in the group treated with s-Flt1 expressing fibroblasts (quantified in Fig. 5*c*, *p* values 0.014). The presence of fibrotic areas in the ES2 tumor could be identified in tumor section (Figs. 5*d* and 5*e*).

Ascites volume was measured and tumor burden was assessed and scored according to amount and spread of tumor nodules (Fig. 5*i*, Supporting Information Table 1). Injection of sFlt expressing fibroblasts resulted in a significant reduction in the ascites volume in the mice, (*p* values 0.0049). Although s-Flt1 expressing fibroblasts injection did not reduce the amount of peritoneal attached tumors, the overall survival of the mice was improved for both ES2 (Fig. 1*f*, *p* values 0.0216) and SKOV3 peritoneal tumor xenografts (Supporting Information Fig. S3, *p* values 0.0126).

The systemic level of s-Flt1 was measured in the blood, showing no difference between mice injected with control or

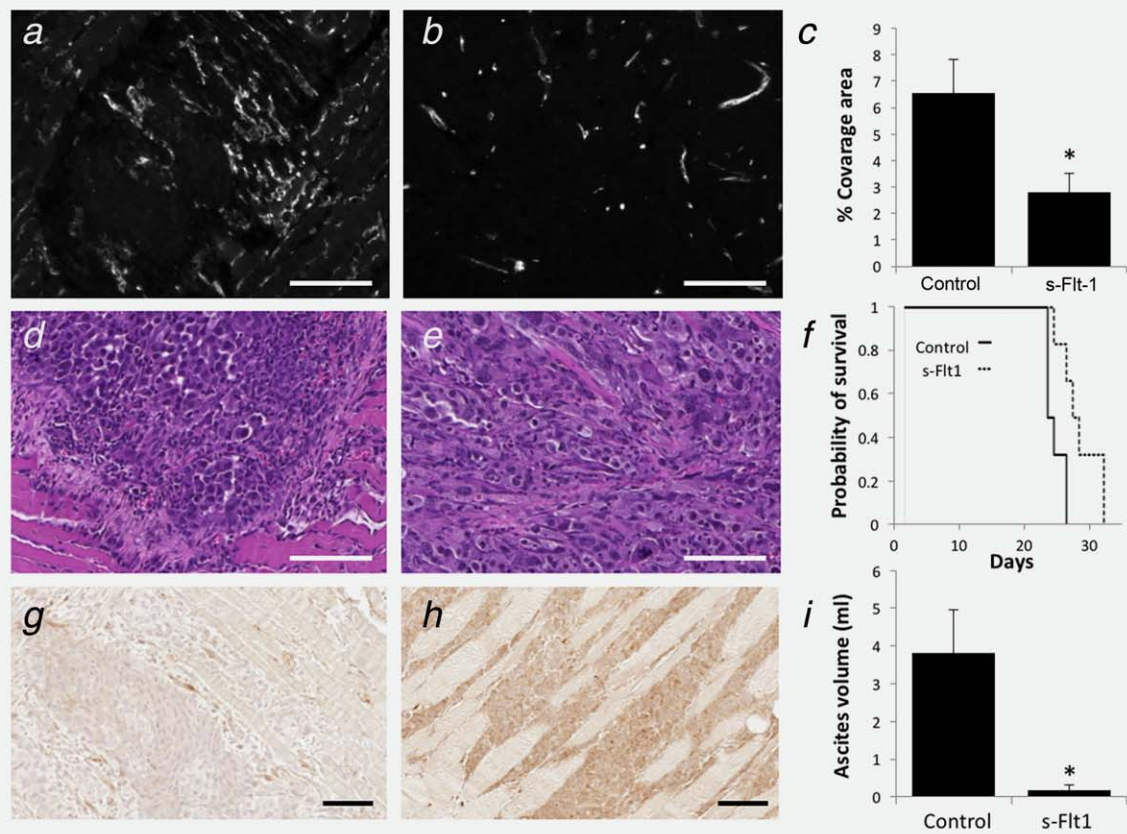**Tumor Immunology and Microenvironment**

Figure 5. s-Flt1 expression by recruited fibroblasts reduced new blood vessels formation of adherent metastases and ascites accumulation. MRC5 fibroblasts expressing control (A,D,G) or s-Flt1 (B,E,H) fibroblasts were injected IP 1 week and again 2 weeks after IP injection of 200 ES2 tumor spheroids. Mice diaphragm was analyzed 21 days post tumor initiation. (a,b) CD34 staining for newly formed blood vessels. Scale bar 100μm. (c) Quantification of the vessels coverage area in tumor attachment sites on the diaphragm (control $n = 7$, s-flt1 $n = 8$, p values 0.033). (d,e) Hematoxylin and eosin (H&E) staining representative images of tumor sites on the diaphragm. G,H s-FLT1 staining Scale bar 100 μm. (f) Kaplan–Meier survival plot of mice treated with control fibroblasts or s-Flt1 expressing fibroblasts (p values 0.0216). (i) Ascites volume was measured with a syringe. Ascites volume is reported as mean ± standard error (control, $n = 7$, s-Flt1, $n = 8$ p-value <0.005).

s-Flt expressing fibroblasts (Supporting Information Fig. S6). On the other hand, staining of the diaphragm region for s-Flt1 confirmed that locally it is more abundant following injection of s-Flt1 expressing fibroblasts (Figs. 5g and 5h).

In summary, we show that s-Flt1 expression by recruited fibroblasts remains localized to the recruiting tumor sites and affect VEGF activity, resulting in reduction of both ascites accumulation and formation of new blood vessels. These results also confirm the possible utility of fibroblasts for cell-based, site-specific delivery of therapeutics.

Discussion

The use of cell-based therapy in cancer was proposed long ago and is a topic of many preclinical and clinical trials. These trials often use immune cells to target the tumor or to activate an autoimmune response.[35,36,39] In this study we demonstrate the feasibility of using fibroblasts cells that specifically home to a preclinical model of ovarian tumor nodules. Endogenous fibroblasts are recruited and activated by ovarian carcinoma tumors in a large amount. As fibroblasts are recruited to the tumor endogenously from local environ-

ment and from the bone marrow, exogenous fibroblasts are only fraction of the total amount of fibroblasts in the tumor. However, the mechanism by which fibroblasts are recruited to the tumor nodules is yet unknown. Mesenchymal stem cells (MSC) were reported to be recruited to tumor microenviroment by inflammatory signals, hypoxia, and various growth factor and cytokines.[43] These signaling pathways may give some clues as to the recruitment of exogenous fibroblasts, however further work is still needed.

Addition of exogenously labeled fibroblasts in our subcutaneous model did not have an inhibitory or stimulatory effect on tumor growth. Similarly, Scherz et al. showed that co-injection of fibroblasts with tumor cells in a solid tumor model did not change tumor progression, as is the same in our model.[44] These findings support the possibility of using fibroblasts cells as a tool in ovarian cancer treatment and detection.

The emerging field of fluorescence guided surgery holds a great promise to be used as a complimentary tool to traditional white light reflectance guided surgery. Fluorescence imaging in surgery has so far been implemented with the use of indocyanine green (ICG) and fluorescein as non-specific

dyes to visualize blood vessels, lymphatic and other structures.[45] Such low MW targeted fluorescent imaging probes can aid in evaluation of surgical margins and identification of residual disease during surgical procedures.[46,47] In this context, the primary treatment offered to ovarian cancer patients is surgery, aimed to remove as much tumor mass as possible, so as to improve treatment outcome. The initial surgery is also the basis for tumor staging and for determining future treatments (chemotherapy regime etc.). In the absence of readily visible lesions, as typical to ovarian carcinoma, random biopsy samples are taken. The ability to enhance the accuracy of visualization of small, possibly otherwise undetected, metastatic nodules by using labeled fibroblasts could therefore improve staging and assist in debulking of tumor and guidance of biopsies, leading to better postoperative selection of therapy for the patient.

In this study, we used two ovarian cell lines (ES2 and SKOV3) in intraperitoneal model for ovarian cancer, and in subcoutenous model previously published the recruitment was demonstrated in MLS and ES2 cell lines. These results suggests that fibroblasts recruitment might be applicable in various types of ovarian cancer.

Tumor angiogenesis has a critical role supporting the growth of solid tumors and is associated with the accumulation of malignant ascites in ovarian carcinoma.[30,31] Angiogenic inhibitors were shown to significantly reduce the accumulation of ascites.[30,48,49] Increase in the peritoneal microvessels permeability was reported to correlate with ascites accumulation both in pre-clinical and clinical data.[50–53] We have demonstrated that recruited fibroblasts are associated with blood vessels *in vivo* and *in vitro,* they can up regulate the expression of pro-angiogenic factors in response to secreted signals from tumor cells. In this study we utilized the specific fibroblasts recruitment to tumor in metastatic model and demonstrated that they can be used efficiently to prevent ascites fluid accumulation by secretion of sFlt-1. Expression of sFlt-1 directly by ovarian cancer cells was previously reported to suppress ascites accumulation in a mouse model,[30] showing the importance of VEGF to ascitic development. Adenovirus infection of muscle to express sFlt-1 was also used as a method to systemically deliver sFlt-1.[54] The local expression of sFLT-1 in the tumor area and not in the circulation reported here indicate that using fibroblasts as a delivery vehicle provides a novel approach for the sustained localized delivery of sFlt-1. This approach can effectively suppress ascites accumulation and may assist in ovarian cancer treatment, while reducing the detrimental side-effects associated with systemic suppression of VEGF such as bowel perforation that may occur in the peritoneal cavity.

Significance

Fibroblasts may be enlisted for ovarian cancer therapy during staging and debulking surgery. We have demonstrated fibroblast recruitment to ovarian cancer spheroids and nodules *in vitro* and *in vivo*. The cancer nodules are mostly of a size which is undetectable by the naked eye. The co-localization of ovarian cancer cells and fibroblasts is very specific with low false negative and false positive events. This may be useful for both staging of cancer level in patients and during debulking surgery. The utility of available fluorescence detection tools for surgery guidance will be enhanced by improved labeling of tumors. Fluorescently labeled fibroblasts may serve as a beacon pointing to the otherwise invisible metastases in the peritoneal cavity of women with ovarian cancer. Moreover, by endowing these cells with expression and release of sFlt-1, these cells can aid in control of angiogenesis and formation of ascitic fluid.

These results and the system described in this study, using pre-clinical mice model for ovarian tumors and human tissue *in vitro,* provide a novel tool to target ovarian tumor metastases both for tumor detection and therapy. The recruited fibroblasts act as delivery vehicles, allowing for the sFlt-1 to be expressed only at the tumor site, inducing localized effect and reducing systemic effects. The presented study serves as a proof of concept of utilization of fibroblast as a biological tool for specific targeting labeling and delivery to tumor metastasis, which can be modified relatively easily to a range of labels and cargo. Further work is needed in order to develop this method to clinical application.

References

1. Siegel R, Naishadham D, Jemal A. Cancer statistics, 2013. *CA: A Cancer J Clin* 2013;63:11–30.
2. Kim A, Ueda Y, Naka T, et al. Therapeutic strategies in epithelial ovarian cancer. *J Exp Clin Cancer Res CR* 2012;31:14
3. Howlader N, Noone A, Krapcho M, et al. SEER Cancer Statistics Review, 1975–2008. Bethesda, MD: National Cancer Institute; 2011. *Also available online Last accessed December 2011;*1.
4. Ozols RF, Bookman MA, Connolly DC, et al. Focus on epithelial ovarian cancer. *Cancer Cell* 2004;5:19–24.
5. Schorge JO, McCann C, Del Carmen MG. Surgical debulking of ovarian cancer: what difference does it make? *Rev Obstetrics Gynecol* 2010;3:111–7.
6. Sugarbaker PH. Management of peritoneal-surface malignancy: the surgeon's role. *Langenbeck's Arch Surg/Deutsche Gesellschaft Fur Chirurgie* 1999;384:576–87.
7. Hirche C, Engel H, Kolios L, et al. An experimental study to evaluate the Fluobeam 800 imaging system for fluorescence-guided lymphatic imaging and sentinel node biopsy. *Surg Innovation* 2013;20:516–23.
8. Keramidas M, Josserand V, Righini CA, et al. Intraoperative near-infrared image-guided surgery for peritoneal carcinomatosis in a preclinical experimental model. *Br J Surg* 2010;97:737–43.
9. Troyan SL, Kianzad V, Gibbs-Strauss SL, et al. The FLARE intraoperative near-infrared fluorescence imaging system: a first-in-human clinical trial in breast cancer sentinel lymph node mapping. *Annals Surg Oncol* 2009;16:2943–52.
10. van Dam GM, Themelis G, Crane LM, et al. Intraoperative tumor-specific fluorescence imaging in ovarian cancer by folate receptor-alpha tar-

geting: first in-human results. *Nat Med* 2011;17:
1315–9.

11. Keereweer S, Kerrebijn JD, van Driel PB, et al.
Optical image-guided surgery–where do we
stand? *Mol Imag Biol* 2011;13:199–207.

12. Cho H, Cho CS, Indig GL, et al. Polymeric
micelles for apoptosis-targeted optical imaging of
cancer and intraoperative surgical guidance. *PloS
One* 2014;9:e89968

13. Tummers QRJG, Hoogstins CES, Gaarenstroom
KN, et al. Intraoperative imaging of folate recep-
tor alpha positive ovarian and breast cancer using
the tumor specific agent EC17ed., 2016.

14. Kalli KR, Oberg AL, Keeney GL, et al. Folate
receptor alpha as a tumor target in epithelial
ovarian cancer. *Gynecol Oncol* 2008;108:619–26.

15. Labiche A, Heutte N, Herlin P, et al. Stromal
compartment as a survival prognostic factor in
advanced ovarian carcinoma. *Int J Gynecol Can-
cer* 2010;20:28–33. 10.1111/
IGC.0b013e3181bda1cb.

16. Ahmed N, Stenvers K. Getting to know ovarian
cancer ascites: opportunities for targeted therapy-
based translational research. *Front Oncol* 2013;3:

17. Kipps E, Tan DS, Kaye SB. Meeting the challenge
of ascites in ovarian cancer: new avenues for
therapy and research. *Nat Rev Cancer* 2013;13:
273–82.

18. Orimo A, Gupta PB, Sgroi DC, et al. Stromal
fibroblasts present in invasive human breast car-
cinomas promote tumor growth and angiogenesis
through elevated SDF-1/CXCL12 secretion. *Cell*
2005;121:335–48.

19. Schauer IG, Sood AK, Mok S, et al. Cancer-asso-
ciated fibroblasts and their putative role in poten-
tiating the initiation and development of
epithelial ovarian cancer. *Neoplasia* 13:393–405.

20. Nagy JA, Brown LF, Senger DR, et al.
Pathogenesis of tumor stroma generation: a criti-
cal role for leaky blood vessels and fibrin deposi-
tion. *Biochimica Et Biophysica Acta* 1989;948:
305–26.

21. Granot D, Addadi Y, Kalchenko V, et al. In vivo
imaging of the systemic recruitment of fibroblasts
to the angiogenic rim of ovarian carcinoma
tumors. *Cancer Res* 2007;67:9180–9.

22. Vandsburger MH, Radoul M, Addadi Y, et al.
Ovarian carcinoma: quantitative biexponential
MR imaging relaxometry reveals the dynamic
recruitment of ferritin-expressing fibroblasts to
the angiogenic rim of tumors. *Radiology* 2013;
268:790–801.

23. Joyce JA. Therapeutic targeting of the tumor
microenvironment. *Cancer Cell* 2005;7:513–20.

24. Micke P, Ostman A. Tumour-stroma interaction:
cancer-associated fibroblasts as novel targets in
anti-cancer therapy? *Lung Cancer* 2004;45 (Suppl
2):S163–75.

25. Francia G, Emmenegger U, Kerbel RS. Tumor-
associated fibroblasts as "Trojan Horse" media-
tors of resistance to anti-VEGF therapy. *Cancer
Cell* 2009;15:3–5.

26. Mesiano S, Ferrara N, Jaffe RB. Role of vascular
endothelial growth factor in ovarian cancer: inhi-
bition of ascites formation by immunoneutraliza-
tion. *Am J Pathol* 1998;153:1249–56.

27. Hiratsuka S, Minowa O, Kuno J, et al. Flt-1 lack-
ing the tyrosine kinase domain is sufficient for
normal development and angiogenesis in mice.
Proc Natl Acad Sci USA 1998;95:9349–54.

28. Kearney JB, Ambler CA, Monaco KA, et al. Vas-
cular endothelial growth factor receptor Flt-1
negatively regulates developmental blood vessel
formation by modulating endothelial cell division.
Blood 2002;99:2397–407.

29. Sela S, Itin A, Natanson-Yaron S, et al. A novel
human-specific soluble vascular endothelial
growth factor receptor 1: cell-type-specific splic-
ing and implications to vascular endothelial
growth factor homeostasis and preeclampsia. *Circ
Res* 2008;102:1566–74.

30. Fischer C, Mazzone M, Jonckx B, et al. FLT1 and
its ligands VEGFB and PlGF: drug targets for
anti-angiogenic therapy? *Nat Rev Cancer* 2008;8:
942–56.

31. Hasumi Y, Mizukami H, Urabe M, et al. Soluble
FLT-1 expression suppresses carcinomatous asci-
tes in nude mice bearing ovarian cancer. *Cancer
Res* 2002;62:2019–23.

32. Laib AM, Bartol A, Alajati A, et al. Spheroid-
based human endothelial cell microvessel forma-
tion in vivo. *Nat Protocols* 2009;4:1202–15.

33. Hobbs S, Jitrapakdee S, Wallace JC. Development
of a bicistronic vector driven by the human poly-
peptide chain elongation factor 1-± promoter for
creation of stable mammalian cell lines that
express very high levels of recombinant proteins.
Biochem Biophys Res Commun 1998;252:368–72.

34. Wiznerowicz M, Fong AZ, Hawley RG, et al.
Development of a double-copy bicistronic retrovi-
ral vector for human gene therapy. *Adv Exp Med
Biol* 1998;451:441–7.

35. Qian X, Wang X, Jin H. Cell transfer therapy for
cancer: past, present, and future. *J Immunol Res*
2014;2014:525913

36. Kershaw MH, Westwood JA, Darcy PK. Gene-
engineered T cells for cancer therapy. *Nat Rev
Cancer* 2013;13:525–41.

37. Cohen B, Addadi Y, Sapoznik S, et al. Transcrip-
tional regulation of vascular endothelial growth
factor C by oxidative and thermal stress is medi-
ated by lens epithelium-derived growth
factor/p75. *Neoplasia (New York, NY)* 2009;11:
921–33.

38. Vandoorne K, Addadi Y, Neeman M. Visualizing
vascular permeability and lymphatic drainage
using labeled serum albumin. *Angiogenesis* 2010;
13:75–85.

39. Kobayashi M, Chiba A Izawa H. The DCvsgatJ-
SoICT, et al. The feasibility and clinical effects of
dendritic cell-based immunotherapy targeting
synthesized peptides for recurrent ovarian cancer.
J Ovarian Res 2014; 7:48

40. Cirri P, Chiarugi P. Cancer associated fibroblasts:
the dark side of the coin. *Am J Cancer Res* 2011;
1:482–97.

41. Gelmini S, Mangoni M, Serio M, et al. The criti-
cal role of SDF-1/CXCR4 axis in cancer and can-
cer stem cells metastasis. *J Endocrinol Invest*
2014;31:809–19.

42. Addadi Y, Moskovits N, Granot D, et al. p53 Sta-
tus in stromal fibroblasts modulates tumor
growth in an SDF1-dependent manner. *Cancer
Res* 2010;70:9650–8.

43. Spaeth E, Klopp A, Dembinski J, et al. Inflamma-
tion and tumor microenvironments: defining the
migratory itinerary of mesenchymal stem cells.
Gene Ther 2008;15:730–8.

44. Scherz-Shouval R, Santagata S, Mendillo Marc L,
et al. The reprogramming of tumor stroma by
HSF1 is a potent enabler of malignancy. *Cell*
2014;158:564–78.

45. Alander JT, Kaartinen I, Laakso A, et al.
A review of indocyanine green fluorescent imag-
ing in surgery. *Int J Biomed Imaging* 2012;2012:
940585

46. Orosco RK, Tsien RY, Nguyen QT. Fluorescence
imaging in surgery. *Biomed Eng IEEE Rev* 2013;6:
178–87.

47. Tran Cao HS, Kaushal S, Metildi CA, et al.
Tumor-specific fluorescence antibody imaging
enables accurate staging laparoscopy in an ortho-
topic model of pancreatic cancer. *Hepato-gastro-
enterology* 2012;59:1994–9.

48. Heuser LS, Taylor SH, Folkman J. Prevention of
carcinomatosis and bloody malignant ascites in
the rat by an inhibitor of angiogenesis. *J Surg Res*
1984;36:244–50.

49. Marme A, Strauss G, Bastert G, et al. Intraperito-
neal bispecific antibody (HEA125xOKT3) therapy
inhibits malignant ascites production in advanced
ovarian carcinoma. *Int J Cancer J Int Du Cancer*
2002;101:183–9.

50. Senger D, Galli S, Dvorak A, et al. Tumor cells
secrete a vascular permeability factor that pro-
motes accumulation of ascites fluid. *Science* 1983;
219:983–5.

51. Garrison RN, Galloway RH, Heuser LS. Mecha-
nisms of malignant ascites production. *J Surg Res*
1987;42:126–32.

52. Garrison RN, Kaelin LD, Galloway RH,
et al. Malignant ascites. Clinical and
experimental observations. *Annals Surg* 1986;203:
644–51.

53. Sherer DM, Eliakim R, Abulafia O. The role of
angiogenesis in the accumulation of peritoneal
fluid in benign conditions and the development
of malignant ascites in the female. *Gynecol
Obstetric Invest* 2000;50:217–24.

54. Takei Y, Mizukami H, Saga Y, et al. Suppression
of ovarian cancer by muscle-mediated expression
of soluble VEGFR-1/Flt-1 using adeno-associated
virus serotype 1-derived vector. *Int J Cancer J Int
Du Cancer* 2007;120:278–84.

Tumor Immunology and Microenvironment